Mitin, Dmitry; Berdnikov, Yury; Vorobyev, Alexandr; Mozharov, Alexey; Raudik, Sergei; Koval, Olga; Neplokh, Vladimir; Moiseev, Eduard; Ilatovskii, Daniil; Nasibulin, Albert G.; Mukhin, Ivan

Optimization of Optoelectronic Properties of Patterned Single-Walled Carbon Nanotube Films

Published in:
ACS Applied Materials and Interfaces

DOI:
10.1021/acsami.0c14783

Published: 09/12/2020

Document Version
Peer-reviewed accepted author manuscript, also known as Final accepted manuscript or Post-print

Optimization of optoelectronic properties of patterned single-walled carbon nanotube films

Dmitry Mitin[*,⸸,‖,‡], *Yury Berdnikov*[#,‡], *Alexandr Vorobyev*[⸸], *Alexey Mozharov*[⸸], *Sergei Raudik*[⸸,†], *Olga Koval*[⸸], *Vladimir Neplokh*[⸸], *Eduard Moiseev*[├], *Daniil Ilatovskii*[†], *Albert G. Nasibulin*[**†,§] *and Ivan Mukhin*[⸸,#]

⸸ Saint Petersburg Academic University, 8 Khlopina, bld. 3A, St. Petersburg 194021, Russia

‖ Peter the Great St. Petersburg Polytechnic University, 29 Politekhnicheskaya, St. Petersburg 195251, Russia

ITMO University, 49 Kronverksky pr., St. Petersburg 197101, Russia

† Skolkovo Institute of Science and Technology, Nobel 3, Moscow 121205, Russia

├ National Research University Higher School of Economics, 16 Soyuza Pechatnikov, St Petersburg 190008, Russia

§ Aalto University, P.O. Box 16100, FI-00076 Aalto, Espoo, Finland.

Corresponding Authors:

*E-mail: mitindm@mail.ru, **E-mail: a.nasibulin@skoltech.ru

KEYWORDS. single-walled carbon nanotubes, patterning, transparent conductive films, flexible transparent electrodes, figure of merit

ABSTRACT. We propose a novel strategy to enhance optoelectrical properties of single-walled carbon nanotube (SWCNT) films for transparent electrode applications by film patterning. First, we theoretically considered the effect of the conducting pattern geometry on the film quality factor and, then, experimentally examined the calculated structures. We extend these results to show that the best characteristics of patterned SWCNT films can be achieved using the combination of initial film properties: low transmittance and high conductivity. The proposed strategy allows the patterned layers of SWCNTs to outperform the widely used indium-tin-oxide electrodes on both flexible and rigid substrates.

Recent development of optoelectronic and photonic technologies for compact devices have introduced new challenges in fabrication of flexible, stretchable, transparent and conductive electrodes [1–3]. A wide range of possible applications includes solar cells [4], light emitting diodes (LEDs) [5–7], touchscreens [1,8,9], "smart" devices, and wearable electronics [2,10]. The typical requirement for these applications is high transmittance in the middle of the visible spectral range and low sheet resistance. A few recent works have recently proposed new approaches, which allowed competing with highly efficient, indium-tin-oxide (ITO) coatings, one of the most developed and spread transparent conductive film (TCF) materials[1,11]. However, poor mechanical properties, high refractivity and price [2,12–14], made researchers and engineers to search for alternative TCFs. Remarkable results were obtained with Cu and Ag nanofibers and nanowires [15], zinc oxide doped with Al and Ga [16,17], conductive polymers as PEDOT:PSS [6,18], metallic grids [10,19], graphene [8], multiwalled and single-walled carbon nanotubes (SWCNTs)[20,21]. The latter is considered to be one of the most promising materials for the ITO replacement due to outstanding mechanical properties, chemical stability, and high intrinsic conductivity [22–28]. SWCNT-based TCFs possess excellent optical properties with no haze[29–31] and low reflectivity[30,31] contrary to metal-oxide materials [31]. However, even the best quality pristine SWCNT films possess quite high sheet resistance ≥300 Ω/□ (at the transmittance of 90%) that limits their potential applicability[32–35]. Doping is the most effective approach to enhance the efficiency of transparent electrodes due to the possibility to tune the electronic structure of the SWCNTs, which results in the increase of the concertation of charge carriers and eliminates the Schottky barriers between SWCNTs with different chirality and metallicity[36]. However, the main drawback of this method is that the doping effect eventually degrades. Hence, the instability in properties stimulates the search of other approaches to produce highly conductive and transparent films performing at the state-of-the-art level.

Recently, Fukaya *et al.* have demonstrated that a film patterning may improve the characteristics of a SWCNT film [9], although no systematic studies of the performance of patterned SWCNT TCFs were reported. Furthermore, the patterned layers demonstrated the performance below ITO values[11]. In general, patterning approach has been established as the strategy to overcome the conductivity-transmittance trade-off for several TCF nanomaterials like polyurethane/metal gratings [37] or transparent conducting oxide grid fingers [38]. However, optimal pattern geometry, especially in the case of SWCNT films, has not been investigated in the literature.

In this work we utilize a patterning approach and carefully examine the processed SWCNT films to enhance their optoelectrical properties beyond the ITO performance. We optimized the trade-off dependence between transparency and film conductivity first theoretically and then confirm the results experimentally. The proposed approach was combined together with continuous films to provide homogenous film conductivity. Our results have demonstrated that flexible SWCNT films can outperform ITO coatings on rigid surfaces.

RESULTS AND DISCUSSION

To evaluate the optoelectronic performance of different materials and to compare a TCF with different thicknesses, we can use the figure of merit (FoM), which is defined as the ratio of conductivity and light absorption [35]:

$$FoM = \frac{\sigma_S}{A} = \frac{1}{AR_S} = -\frac{1}{\log(T)\cdot R_S}, \quad (1)$$

where σ_S and R_S are the sheet conductivity and resistance, respectively; A and T are the absorbance and transmittance at 550 nm wavelength, respectively. Among other FoMs, eq. (1) is the simplest to be used; however, a value of FoM is not always straightforward and requires to know the figures for other materials to compare the film performance. Therefore, to overcome this problem we utilize an equivalent sheet resistance, R_{90}, which is the sheet resistance of a film with the 90% transmittance at 550 nm:

$$R_{90} = \frac{1}{FoM\cdot log(10/9)}. \quad (2)$$

As the best up to now, recent studies devoted to the transparent conductors based on SWCNT films have reported values of R_{90} = 17-42 Ω/□[21,39–41], comparable with flexible ITO layers (R_{90} = 36 Ω/□ [42]), but still higher than 10 Ω/□ [43] corresponding to ITO films on a rigid substrate.

We considered the grids made of SWCNT films with the period of p and width of the stripes of w illustrated in Figure 1(a)-(d). To characterize grids with a different cell shape, we introduce the filling factor of the surface area covered by the grid as $f = 1-(p-w)^2/p^2$. In these terms, the grid transmittance, T, is the function of transmittance of a continuous SWCNT film before patterning, T_0:

$$T = 1 - f + f\,T_0, \tag{3}$$

assuming 100% transmittance of the area between stripes.

The sheet resistance of the square grid can be estimated as a function of the sheet resistance of a continuous layer of the same material before patterning, R_0:

$$R_s = R_0 \frac{p}{w} = \frac{R_0}{1-\sqrt{1-f}}\,. \tag{4}$$

The right-hand side of eq. (4) is universal and applicable to grids with various cell shapes, as we show in Supporting Information (section S1).

Previous studies have confirmed that the transmittance of the continuous SWCNT layer follows the Lambert-Beer law and relates to its sheet resistance as [9,18,35,44]:

$$T_0 = exp\,(-\alpha\rho/R_0), \tag{5}$$

where α is the effective absorption coefficient, ρ is the resistivity of the SWCNT layer. Using eqs. (3) - (5), we obtain the correlation between T and R_s for the patterned SWCNT layer:

$$T = 1 - f + f\,exp\left(-\frac{\alpha\rho}{R_s\left(1-\sqrt{1-f}\right)}\right). \tag{6}$$

The dependences of $T(R_s)$ given by eq. (6) are plotted for different f values and fixed $\alpha\rho = 12.9$ in Figure 1(e). This value for $\alpha\rho$ was calculated using eq. (5) and experimental data: $T_0 = 0.95$ and $R_0 = 227\ \Omega/\square$ measured for continuous doped SWCNT films examined in this paper. We note that for a continuous SWCNT film (i.e. at $f = 1$) the function of $T(R_s)$ turns into the correlation of $T_0(R_0)$ described by eq. (5). Meanwhile, for $f < 1$, the $T(R_s)$ curve intersects with the $T_0(R_0)$ dependence. The left side of the $T(R_s)$ curve corresponds to the patterned SWCNT layers with the improved transmittance in comparison to a continuous layer of the same sheet resistance. And the right side from the intersection of the $T(R_s)$ curve corresponds to the transmittance lower than the original transmittance, T_0, for the same sheet resistance, which has no any practical use. Therefore, the $T(R_s)$ curve in Figure 1(e) delineates the clean region related to the patterned SWCNT layers with the enhanced optoelectronic characteristics and shadowed area with superiority of the continuous film. The boundary between these two regions can be found by solving the equation at the intersection of $T(R_s)$ and $T_0(R_0)$:

$$1 - f + f\,T_0 = T_0^{1-\sqrt{1-f}}. \tag{7}$$

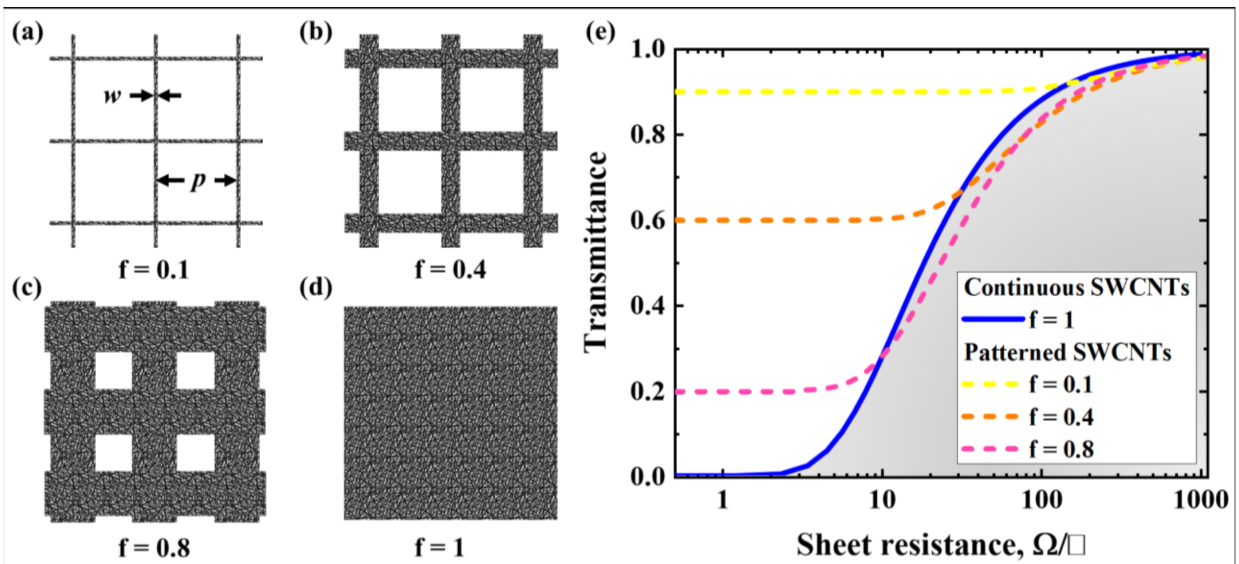

Figure 1. (a)-(d) Schematics of the patterned SWCNT grid for $f = 0.1$, 0.4, 0.8, and 1, respectively; (e) Transmittance of patterned and continuous SWCNT layers as a function of sheet resistance. Clean area corresponds to the conditions, where the patterned films demonstrate improvement of optoelectronic properties, and the shadowed one is the area of superiority of the continuous film.

Eq. (7) is expressed in terms of f and R_s, however, it could be rewritten as a function of other parameters using eq. (3) and eq. (4), as discussed in Supporting Information (section S2).

Unfortunately, eq. (7) has no precise analytical solution and can be solved only numerically or approximated analytically, which we discuss in detail in Supporting Information (section S3).

From a practical point of view, high TCF transmittance is crucial for such applications as LEDs, solar cells and touch sensors [11]. Therefore, next we discuss the choice of T_0 to fabricate TCF with an arbitrary transmittance, T. The filling factor can be found as $f = (1-T)/(1-T_0)$ and the sheet resistance as:

$$R_s = \frac{-\alpha\rho/\ln T_0}{1-\sqrt{1-\frac{1-T}{1-T_0}}}. \tag{8}$$

Figure 2 shows the non-monotonic sheet resistance, R_s, dependence on the initial transmittance, T_0, calculated according to eq. (8) at fixed final transmittances of T = 0.90 and 0.95. Similar to Figure 1(c), the regions where patterning improves or worsens the performance correspond to clean and shadowed areas. The dotted line represents the solution of eq. (7) and separates these two regions. The dashed vertical lines mark the resistance of the thin unpatterned SWCNT films with the transmittances of 0.90 and 0.95. As clearly seen from the figure, the patterned layers prepared of films with the initial transmittance of $T_0 < 0.2$ demonstrate the sheet resistance values lower than that of a continuous SWCNT layer of the same transmittance of 0.90 and 0.95. More generally, we can conclude that patterning of SWCNT layers with low transmittance is expected to improve their performance beyond the above-mentioned trade-off. Next, we give the experimental confirmation of this theoretical conclusion, further addressing the possibility to outperform ITO coatings.

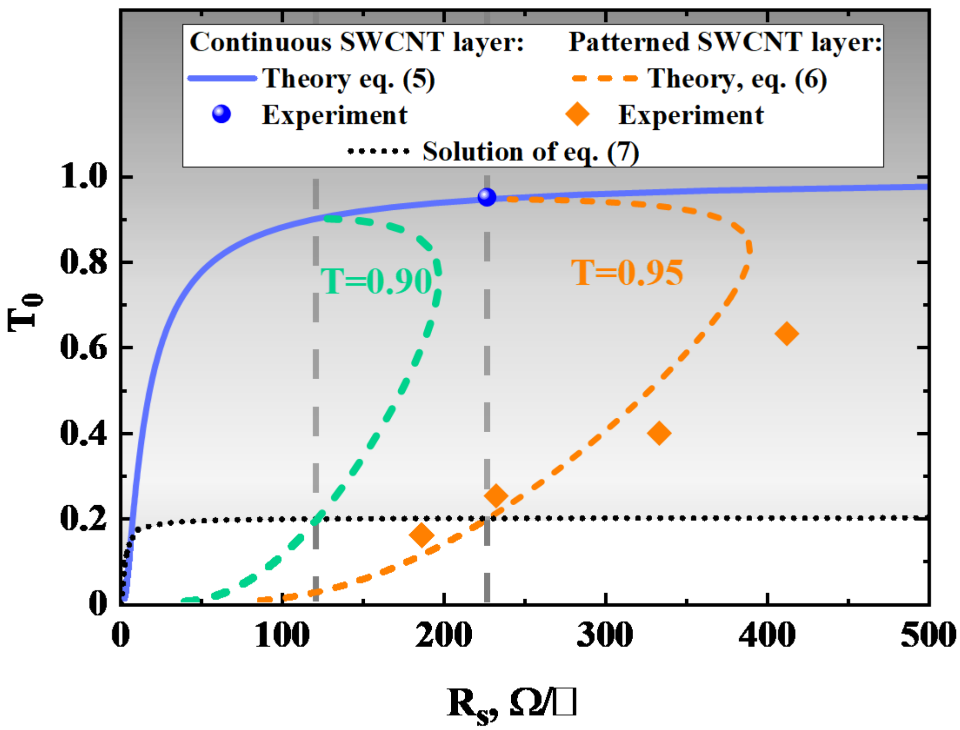

Figure 2. Dependence of the sheet resistance of patterned (dashed line) and continuous (solid line) SWCNT films on the transmittance of SWCNT layers before the patterning. Symbols represent the experimentally obtained data. The dashed line shows the dependence given by eq. (6) at target transmittances of 90% and 95%. The dotted line shows the solution of eq. (7). The clean area below the dotted line is the region of improved optoelectronic properties, the shadowed one is that of worsened properties of the patterned films.

Continuous layers of randomly oriented SWCNTs were produced by the following sequence: SWCNTs were synthesized by the aerosol chemical vapor deposition (CVD) method, deposited in the form of thin films on filters and then transferred on a quartz substrate, doped and then patterned using a combination of optical laser lithography and oxygen plasma etching. The details of the CVD synthesis, doping and patterning procedure are described in section Methods.

The effects of lithographic processing, etching and doping of the SWCNTs were examined with Raman spectroscopy. Figure 3 shows the Raman spectra acquired after each step of the SWCNT film processing. All the spectra demonstrate the main vibrational modes related to SWCNTs: D- and G- bands and radial breathing modes (RBMs) [45,46]. The shape and intensity of Raman peaks do not practically change after every step of the fabrication of a patterned SWCNT film, except a slight decrease in the RBM peak intensity after the $HAuCl_4$ treatment. This means that no significant changes occur with the SWCNT structure during the patterning process.

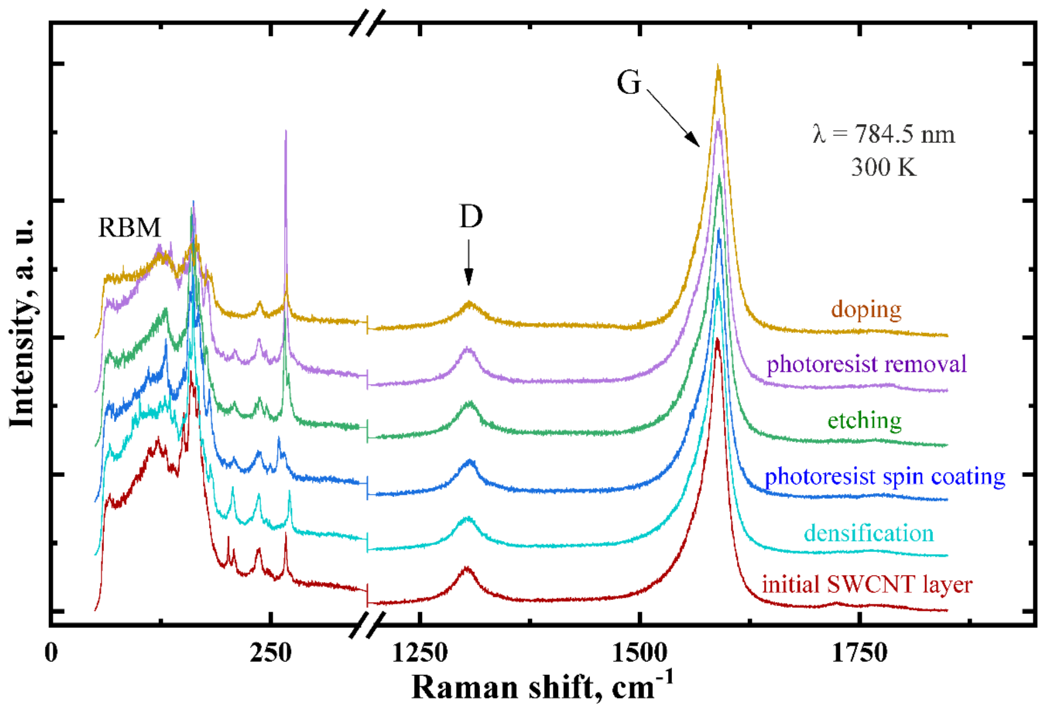

Figure 3. Room-temperature Raman spectra (λ = 784.5 nm) of SWCNT films after every step of the patterned film fabrication (all spectra are normalized to the G-band intensity).

For the patterning process we used a set of SWCNT films with thicknesses of 90, 180, 270 and 360 nm and correspondingly measured transmittances of T_0 = 0.63, 0.40, 0.25 and 0.16 (at 550 nm). The pattern linewidths were chosen aiming for the target transmittance of $T = 0.95$. The filling factor values were calculated from 0.06 to 0.14 according to eq. (3), which corresponds to the linewidth change from 8 to 15 μm at a constant period of 240 μm. Figure 4 compares the transmittance spectra of the patterned (dashed lines) and unpatterned (solid lines) SWCNT layers. The patterned films show the measured transmittance (at 550 nm) close to the target value of 0.95. We noticed the drop of transmittance in the ultraviolet range, typical for unpatterned films, is lower for the patterned TCFs. We also note that the experimentally obtained values of transmittances (at 550 nm wavelength) and sheet resistances of patterned films match the theoretically predicted dependences with the transmittance deviation of ± 0.5%, as shown in Figure 2. However, the drop in the measured transmission in the UV region is more prominent compared to theoretical predictions. This phenomenon can be explained by considering the residue of photoresist on the substrates with patterned films. Indeed, the thin layer of photoresist can significantly increase the light absorption, especially in the UV region.

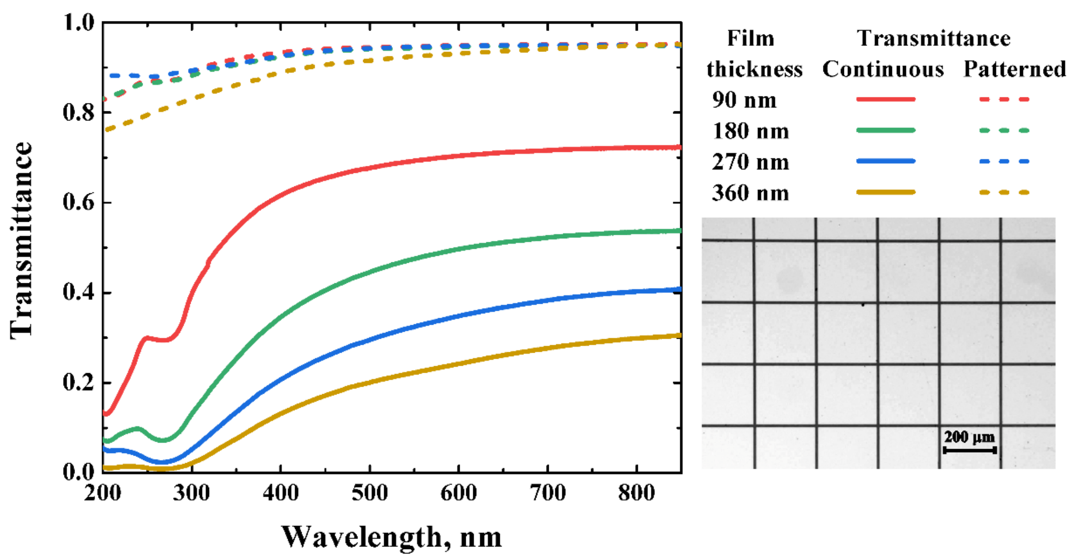

Figure 4. Optical transmittance spectra of patterned and continuous SWCNT films. The inset demonstrates the optical microscopy image of a patterned SWCNT film on a quartz substrate with the thickness of 90 nm, linewidth of 8 μm, cell period of 240 μm with the filling factor of 0.06. The spectra were measured against the quartz substrate.

Unlike traditional continuous thin films, the resistance of the patterned SWCNT TCF does not always scale linearly with the sample thickness. Thin films or narrow stripes of SWCNT networks are known to suffer from an increase of resistance due to the lack of contacts between tubes when approaching the percolation threshold [44,47], which we have not considered in our model. Therefore, a series of experiments was carried out to examined how the patterning affects the conductivity of SWCNT networks. A set of SWCNT stripes with widths of 1-100 μm and lengths of 10-1000 μm was prepared following the same lithography and etching procedure as described in section Methods. Figure 5 (a) shows the optical microscopy image of the SWCNT stripes with Cr/Au contacts. The resistances of SWCNT stripes were extracted from the I-V characteristics. All the measured I-V curves have shown linear or almost linear dependence revealing ohmic or close to ohmic behavior of SWCNT-Au contact, as illustrated by several typical examples in Supporting Information (section S4).

Figures 5 (b) and (c) show the normalized stripe resistances, R, as a function of the stripe length and width, correspondingly. The $R \times w$ dependences scale almost linearly (the scaling exponent is about 0.95) at the lengths above 50 μm. However, as expected the points corresponding to the shortest measured stripes with the length of 10 μm do not follow the linear scaling law. Previously, similar behavior was described to correspond to the transition from ballistic to diffusive transport in randomly oriented networks [48–50]. Figure 5 (c) shows that the measured resistances scale as w^{-1} which is typical for SWCNT networks far above the percolation threshold [50]. Therefore, in patterns with the linewidth above 1 μm and the cell size above 50 μm the random character of SWCNT networks can be neglected.

We note that SWCNT layers remain flexible after patterning. The results of bending tests of patterned SWCNT layer on flexible polydimethylsiloxane (PDMS) substrate are given in Supporting Information (section S5).

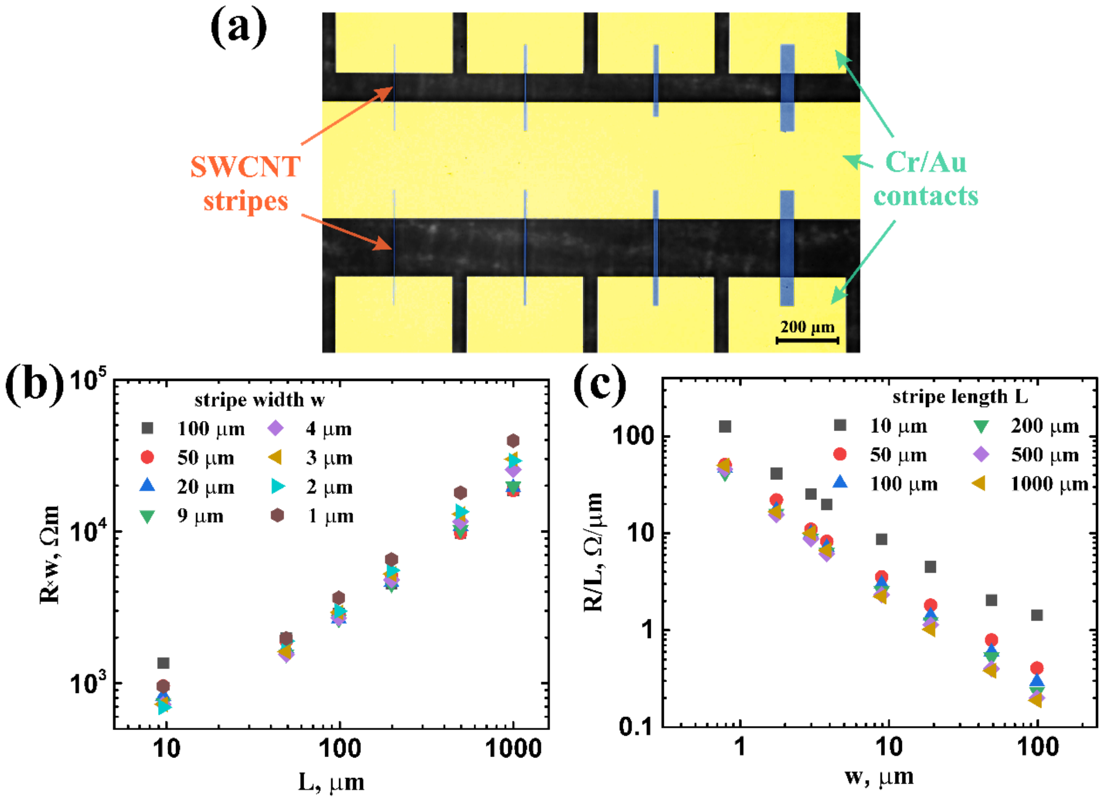

Figure 5. (a) Optical microscopy image in false colors of the set of SWCNT stripes (colored in blue) with Cr/Au contacts (colored in yellow) on quartz substrate; (b) the stripe resistances multiplied by its width as the functions of the stripe length; (c) the stripe resistances divided by its length as the functions of the stripe width.

The correlation between transmittance, T, and sheet resistance, R, is correspondingly given either by eq. (5) or by eq. (6) for continuous and patterned SWCNT films. Figure 6 shows FoM and R_{90} values plotted as functions of T_0 for continuous (solid lines) and patterned (dashed lines) SWCNT layers at fixed T. The diamond symbols in Figure 6 demonstrate the experimentally obtained values of R_{90} for the patterned SWCNT layers with the 95% transparency. The best experimentally observed results for the continuous SWCNT films (R_{90} = 17-42 Ω/□[21,39–41]) are marked by the star and pentagon marks.

In our experiments the resistance of the SWCNT films decreases inversely proportional to their thickness from 90 to 360 nm, while the transmittance of the films dropped from T_0 = 0.63 to 0.16. Nevertheless, the SWCNT film patterning provides high transmittance values even in the case of initially thick layers. A similar patterning strategy can be used for the state-of-the-art SWCNT films (R_{90} = 17-42 Ω/□[21,39–41]). The estimated FoM and R_{90} values for the patterned state-of-the-art SWCNT films correspond to the green region between dashed lines in Figure 6.

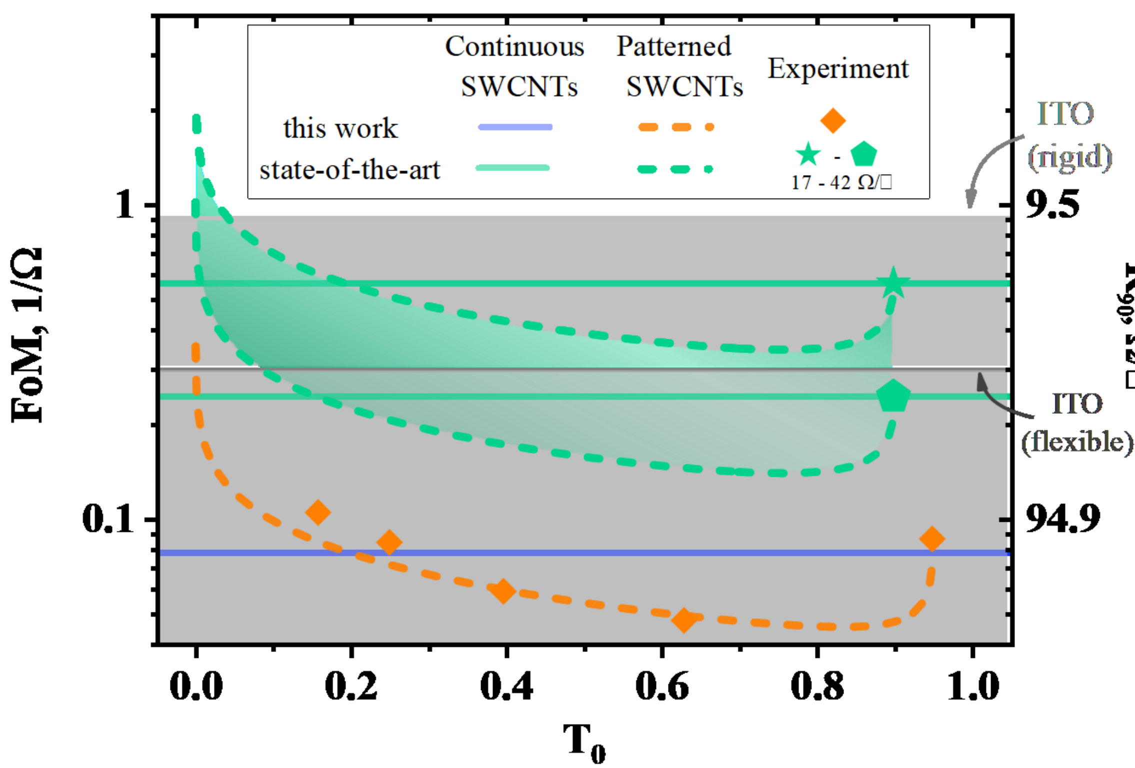

Figure 6. Theoretical dependences (dashed lines) and experimentally based values (symbols) of the TCF figure of merit and equivalent sheet resistance for 90% SWCNT films. The area shaded

with green color shows the predicted FoM and R_{90} of patterned SWCNT TCF corresponding to the state-of-the-art in SWCNT synthesis.

Patterning of SWCNT layers first results in a rapid increase in the R_{90} values with T_0 decrease, and then the patterned SWCNT films show considerably lower R_{90} values when compared to the continuous or patterned layers with high T_0. Therefore, patterning of SWCNT films was concluded to be a reliable approach to overcome the trade-off between resistance and transmittance of the continuous SWCNT layer. The improvement of the patterned layers can be achieved using SWCNT films with low initial transmittance, T_0, and high conductivity.

As can be seen, R_{90} values of patterned layers with an initially low transmittances might achieve 10 Ω/□, which is comparable with the best results for ITO continuous layers on rigid substrates. At the limit of low transmittance, eq. (3) can be reduced to $T \simeq 1 - f$. In this case $w/p \simeq 1 - \sqrt{T}$, which gives the ratio of about 0.05 for the 90% transmittance and about 0.02 for the 95% transmittance. Therefore, the minimal experimentally obtained linewidth of 1 μm gives the estimated lower limit for the grid period between 20 and 50 μm.

However, the use of patterned electrodes can be inefficient in the structures with the carrier mean free path below the grid period[51]. In this case, the patterned layers may be effectively combined with highly transparent continuous thin SWCNT films. The transmittance and resistance of these TCFs can be estimated as $T = T_{patt} \cdot T_{cont}$ and $R^{-1} = R_{patt}^{-1} + R_{cont}^{-1}$, respectively. Here, T_{patt} and R_{patt} are the transmittance and the sheet resistance of the patterned layers; T_{cont} and R_{cont} are the transmittance and the sheet resistance of the continuous film. Thus, we evaluate the FoM of the bilayered TCF as a function of T_{cont} and T_0 of the patterned layer. Figure 7 shows that the maximal FoM (and minimal R_{90}) can be obtained for the combination of a highly transparent continuous layer and a patterned layer made of highly conductive SWCNTs. We note here that the

FoM of the bilayered structure is slightly lower than the FoM of the single patterned layer, nevertheless, the maximum value is still comparable with the best results for ITO. Meantime, SWCNT films have a potential for superior flexibility and stretchability, which opens new avenues for commercial applications beyond the ITO.

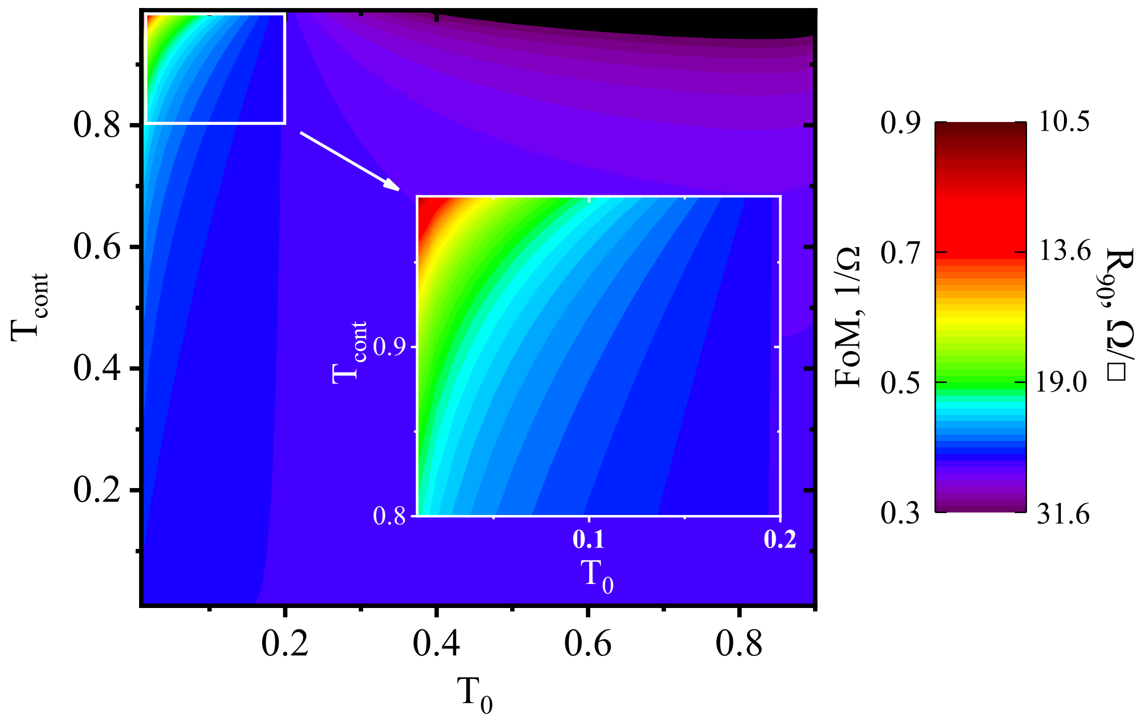

Figure 7. Theoretical calculations of the figure of merit and the equivalent resistance for the combination of patterned and continuous bilayered TCF as a dependence of transmittance of continuous layer T_{cont} and transmittance of original film, T_0.

CONCLUSIONS

We have shown that patterning of SWCNT films is an effective approach to overcome the high transmittance and conductivity trade-off limitations for TCFs. We have presented the model predicting the transmittance and sheet resistance of patterned SWCNT films and demonstrated the consistency of characteristics with the experimental results. We have shown that our fabricaion procedure for patterning using the combination of optical laser lithography and dry etching in an oxygen plasma causes no significant change in SWCNT structure or composition. The systematic studies of the SWCNT patterns revealed the negligible role of random orientation of nanotube networks in SWCNT patterns with linewidth above 1 μm and stripe length above 50 μm. Furthermore, the produced patterned layers show flat transmittance spectra and only a slight decrease in the UV range instead of sharp decline observed in the continuous SWCNT films.

Our theoretical results were extended to analyze the performance of patterned SWCNT films in terms of FoM and R_{90} equivalent sheet resistance. We conclude that patterned SWCNT TCFs with low initial transmittance and high conductivity show superior characteristics in comparison to continuous SWCNT films. We also have investigated the approach based on the combination of a highly transparent continuous film and a highly conductive patterned layer, which can be used in structures with low charge carrier mean free path. Moreover, we have demonstrated that the patterned SWCNT layers solely, as well as in combination with thin continuous films, can outperform the ITO electrodes on both flexible and rigid substrates. We believe that the proposed strategies pave the way for efficient and extended functionality of TCFs on the basis of patterned SWCNT films.

METHODS

CVD synthesis and doping

Films of randomly oriented SWCNTs synthesized by the aerosol chemical vapor deposition (CVD) method were deposited on a nitrocellulose filter at the outlet of the reactor as previously described elsewhere [52,53]. Prior to patterning, the films of SWCNTs were transferred either onto a clean quartz substrate or on a substrate with pre-deposited metallic contacts.

Cr/Au (5/70 nm) contacts were deposited on quartz substrates before the SWCNT transfer by electron-beam physical vapor deposition (for Cr) and thermal evaporation (for Au) using Boc Edwards (UK) Auto 500 setup operating at 5×10^{-6} mbar. Prior to the deposition of metals, the surface of the quartz substrate was cleaned sequentially in acetone, deionized water, isopropyl alcohol and again in deionized water using an ultrasonic bath.

After the deposition of Cr/Au contacts, the SWCNT films were transferred onto the quartz substrates, processed with isopropyl alcohol for densification and then doped in tetrachloroauric (III) acid trihydrate ($HAuCl_4{\cdot}3H_2O$ ACROS Organics) dissolved in ethanol (EtOH; 99.5%, ETAX)[21].

Patterning of SWCNT layers

The patterns of SWCNTs were produced using a combination of optical laser lithography and dry etching in an oxygen plasma. We have used the laser lithography system Heidelberg Instruments Mikrotechnik DWL 66 FS setup (Germany) with AZ MIR 701 photoresist (MicroChemicals GmbH) and AZ 726 MIF developer (MicroChemicals GmbH). The following dry etching was performed in Plasma System V 15-G (Germany) at MW-power of 400 W (O_2 flux 60 ml/min, 3 Pa) during 360, 420, 480 and 540 sec for 90, 180, 270 and 360 nm SWCNT thickness, correspondingly. The grids of SWCNT networks were masked by photoresist during the etching. To ensure uniform grid transmittance of T = 95% of patterned SWCNT layers, we used different width of the stripes from 8 to 15 μm, while the cell period remained constant (~240 μm).

Raman spectroscopy

Raman spectroscopy was performed using the Horiba (Japan) LabRam HR800 system with backscattering collection geometry. The measurements were carried out at room temperature (300K) and resonance conditions with λ = 784.5 nm (1.58 eV) diode-pumped solid-state laser operating in a continuous wave regime.

ASSOCIATED CONTENT

Supporting Information.

Additional materials in Supporting Information. Section S1 gives the model extension to the cases of triangle and hexagonal shapes of grid cell. Section S2 discuss the dependence of patterned film transmittance as a function of the filling factor. Section S3 considers the analytical solution of eq. (7) within a linear approximation. Section S4 includes I-V characteristics of patterned SWCNT layers. Section S5 reports the results of the bending tests of patterned SWCNT layers.

AUTHOR INFORMATION

Corresponding Author

*E-mail: mitindm@mail.ru

**E-mail: a.nasibulin@skoltech.ru

Author Contributions

The manuscript was written through contributions of all authors. All authors have given approval to the final version of the manuscript. ‡These authors contributed equally.

ACKNOWLEDGMENT

The reported study on the SWCNT sheet resistance and transparency modelling was funded by RFBR, project number 19-38-60008. S.R. acknowledge the Russian Science Foundation for support of the metal contacts fabrication and IV-investigations (project # 19-79-00074). A.G.N. and D.I. acknowledge the Russian Science Foundation for the support (synthesis and doping of SWCNTs) by project # 17-19-01787. The authors thank Saint Petersburg State University Center for optical and laser materials research for SWCNTs transmission spectra measurements.

ABBREVIATIONS

SWCNT: single-walled carbon nanotube; TCF: transparent conductive film; ITO: indium-tin-oxide; FoM: figure of merit; CVD: chemical vapor deposition; LED: light-emitting diode.

REFERENCES

(1) McLellan, K.; Yoon, Y.; Leung, S. N.; Ko, S. H. Recent Progress in Transparent Conductors Based on Nanomaterials: Advancements and Challenges. *Adv. Mater. Technol.* **2020**, *5* (4), 1900939. https://doi.org/10.1002/admt.201900939.

(2) Wang, X.; Liu, Z.; Zhang, T. Flexible Sensing Electronics for Wearable/Attachable Health Monitoring. *Small* **2017**, *13* (25), 1–19. https://doi.org/10.1002/smll.201602790.

(3) Morales-Masis, M.; De Wolf, S.; Woods-Robinson, R.; Ager, J. W.; Ballif, C. Transparent Electrodes for Efficient Optoelectronics. *Adv. Electron. Mater.* **2017**, *3* (5), 1600529. https://doi.org/10.1002/aelm.201600529.

(4) Mitin, D. M.; Bolshakov, A. D.; Neplokh, V.; Mozharov, A. M.; Raudik, S. A.; Fedorov, V. V.; Shugurov, K. Y.; Mikhailovskii, V. Y.; Rajanna, P. M.; Fedorov, F. S.; Nasibulin, A. G.; Mukhin, I. S. Novel Design Strategy for GaAs-based Solar Cell by Application of Single-walled Carbon Nanotubes Topmost Layer. *Energy Sci. Eng.* **2020**, *8* (8), 2938–2945.

https://doi.org/10.1002/ese3.713.

(5) Han, T.-H.; Jeong, S.-H.; Lee, Y.; Seo, H.-K.; Kwon, S.-J.; Park, M.-H.; Lee, T.-W. Flexible Transparent Electrodes for Organic Light-Emitting Diodes. *J. Inf. Disp.* **2015**, *16* (2), 71–84. https://doi.org/10.1080/15980316.2015.1016127.

(6) Naka, S. Transparent Electrodes for Organic Light-Emitting Diodes. In *Transparent Conductive Materials*; Wiley-VCH Verlag GmbH & Co. KGaA: Weinheim, Germany, 2018; pp 301–315. https://doi.org/10.1002/9783527804603.ch5_2.

(7) Kang, C. H.; Shen, C.; M. Saheed, M. S.; Mohamed, N. M.; Ng, T. K.; Ooi, B. S.; Burhanudin, Z. A. Carbon Nanotube-Graphene Composite Film as Transparent Conductive Electrode for GaN-Based Light-Emitting Diodes. *Appl. Phys. Lett.* **2016**, *109* (8), 081902. https://doi.org/10.1063/1.4961667.

(8) López-Naranjo, E. J.; González-Ortiz, L. J.; Apátiga, L. M.; Rivera-Muñoz, E. M.; Manzano-Ramírez, A. Transparent Electrodes: A Review of the Use of Carbon-Based Nanomaterials. *J. Nanomater.* **2016**, *2016*, 1–12. https://doi.org/10.1155/2016/4928365.

(9) Fukaya, N.; Kim, D. Y.; Kishimoto, S.; Noda, S.; Ohno, Y.; Engineering, Q.; Chemistry, A. One-Step Sub-10 μ m Patterning of Carbon-Nanotube Thin Films For. *ACS Nano* **2014**, *8* (4), 3285–3293.

(10) An, B. W.; Gwak, E.-J.; Kim, K.; Kim, Y.-C.; Jang, J.; Kim, J.-Y.; Park, J.-U. Stretchable, Transparent Electrodes as Wearable Heaters Using Nanotrough Networks of Metallic Glasses with Superior Mechanical Properties and Thermal Stability. *Nano Lett.* **2016**, *16* (1), 471–478. https://doi.org/10.1021/acs.nanolett.5b04134.

(11) Jiang, S.; Hou, P.-X.; Liu, C.; Cheng, H.-M. High-Performance Single-Wall Carbon Nanotube Transparent Conductive Films. *J. Mater. Sci. Technol.* **2019**, *35* (11), 2447–2462. https://doi.org/10.1016/j.jmst.2019.07.011.

(12) Gao, M. Z.; Job, R.; Xue, D. S.; Fahrner, W. R. Thickness Dependence of Resistivity and Optical Reflectance of ITO Films. *Chinese Phys. Lett.* **2008**, *25* (4), 1380–1383. https://doi.org/10.1088/0256-307X/25/4/059.

(13) Hofmann, A. I.; Cloutet, E.; Hadziioannou, G. Materials for Transparent Electrodes: From Metal Oxides to Organic Alternatives. *Adv. Electron. Mater.* **2018**, *4* (10), 1700412. https://doi.org/10.1002/aelm.201700412.

(14) Kumar, A.; Zhou, C. The Race To Replace Tin-Doped Indium Oxide: Which Material Will Win? *ACS Nano* **2010**, *4* (1), 11–14. https://doi.org/10.1021/nn901903b.

(15) Park, J.; Hyun, B. G.; An, B. W.; Im, H.-G.; Park, Y.-G.; Jang, J.; Park, J.-U.; Bae, B.-S. Flexible Transparent Conductive Films with High Performance and Reliability Using Hybrid Structures of Continuous Metal Nanofiber Networks for Flexible Optoelectronics. *ACS Appl. Mater. Interfaces* **2017**, *9* (24), 20299–20305. https://doi.org/10.1021/acsami.7b04314.

(16) Choi, K.-H.; Nam, H.-J.; Jeong, J.-A.; Cho, S.-W.; Kim, H.-K.; Kang, J.-W.; Kim, D.-G.; Cho, W.-J. Highly Flexible and Transparent InZnSnOx∕Ag∕InZnSnOx Multilayer Electrode for Flexible Organic Light Emitting Diodes. *Appl. Phys. Lett.* **2008**, *92* (22), 223302. https://doi.org/10.1063/1.2937845.

(17) Ellmer, K. Past Achievements and Future Challenges in the Development of Optically

Transparent Electrodes. *Nat. Photonics* **2012**, *6* (12), 809–817. https://doi.org/10.1038/nphoton.2012.282.

(18) He, X.; He, R.; Lan, Q.; Wu, W.; Duan, F.; Xiao, J.; Zhang, M.; Zeng, Q.; Wu, J.; Liu, J. Screen-Printed Fabrication of PEDOT:PSS/Silver Nanowire Composite Films for Transparent Heaters. *Materials (Basel).* **2017**, *10* (3), 220. https://doi.org/10.3390/ma10030220.

(19) Huang, S.; Liu, Y.; Guo, C. F.; Ren, Z. A Highly Stretchable and Fatigue-Free Transparent Electrode Based on an In-Plane Buckled Au Nanotrough Network. *Adv. Electron. Mater.* **2017**, *3* (3), 1600534. https://doi.org/10.1002/aelm.201600534.

(20) Aloui, W.; Ltaief, A.; Bouazizi, A. Transparent and Conductive Multi Walled Carbon Nanotubes Flexible Electrodes for Optoelectronic Applications. *Superlattices Microstruct.* **2013**, *64*, 581–589. https://doi.org/10.1016/j.spmi.2013.10.027.

(21) Tsapenko, A. P.; Goldt, A. E.; Shulga, E.; Popov, Z. I.; Maslakov, K. I.; Anisimov, A. S.; Sorokin, P. B.; Nasibulin, A. G. Highly Conductive and Transparent Films of HAuCl4-Doped Single-Walled Carbon Nanotubes for Flexible Applications. *Carbon N. Y.* **2018**, *130*, 448–457. https://doi.org/10.1016/j.carbon.2018.01.016.

(22) Wu, Z.; Chen, Z.; Du, X.; Logan, J.; Sippel, J.; Nikolou, M.; Kamaras, K.; Reynolds, J.; Tanner, D.; Hebard, A.; Rinzler, A. G. Transparent, Conductive Carbon Nanotube Films. *Science (80-.).* **2004**, *305* (5688), 1273–1276. https://doi.org/10.1126/science.1101243.

(23) Ostfeld, A. E.; Catheline, A.; Ligsay, K.; Kim, K. C.; Chen, Z.; Facchetti, A.; Fogden, S.; Arias, A. C. Single-Walled Carbon Nanotube Transparent Conductive Films Fabricated by

Reductive Dissolution and Spray Coating for Organic Photovoltaics. *Appl. Phys. Lett.* **2014**, *105* (25). https://doi.org/10.1063/1.4904940.

(24) Gilshteyn, E. P.; Lin, S.; Kondrashov, V. A.; Kopylova, D. S.; Tsapenko, A. P.; Anisimov, A. S.; Hart, A. J.; Zhao, X.; Nasibulin, A. G. A One-Step Method of Hydrogel Modification by Single-Walled Carbon Nanotubes for Highly Stretchable and Transparent Electronics. *ACS Appl. Mater. Interfaces* **2018**, *10* (33), 28069–28075. https://doi.org/10.1021/acsami.8b08409.

(25) Sun, D.; Timmermans, M. Y.; Tian, Y.; Nasibulin, A. G.; Kauppinen, E. I.; Kishimoto, S.; Mizutani, T.; Ohno, Y. Flexible High-Performance Carbon Nanotube Integrated Circuits. *Nat. Nanotechnol.* **2011**, *6* (3), 156–161. https://doi.org/10.1038/nnano.2011.1.

(26) Aguirre, C. M.; Auvray, S.; Pigeon, S.; Izquierdo, R.; Desjardins, P.; Martel, R. Carbon Nanotube Sheets as Electrodes in Organic Light-Emitting Diodes. *Appl. Phys. Lett.* **2006**, *88* (18). https://doi.org/10.1063/1.2199461.

(27) Kaskela, A.; Laiho, P.; Fukaya, N.; Mustonen, K.; Susi, T.; Jiang, H.; Houbenov, N.; Ohno, Y.; Kauppinen, E. I. Highly Individual SWCNTs for High Performance Thin Film Electronics. *Carbon N. Y.* **2016**, *103*, 228–234. https://doi.org/10.1016/j.carbon.2016.02.099.

(28) Nasibulin, A. G.; Kaskela, A.; Mustonen, K.; Anisimov, A. S.; Ruiz, V.; Rackauskas, S.; Timmermans, M. Y.; Pudas, M.; Aitchison, B. Multifunctional Free-Standing Single-Walled Carbon Nanotube Films. **2011**, 3214–3221.

(29) Preston, C.; Xu, Y.; Han, X.; Munday, J. N.; Hu, L. Optical Haze of Transparent and

Conductive Silver Nanowire Films. *Nano Res.* **2013**, *6* (7), 461–468. https://doi.org/10.1007/s12274-013-0323-9.

(30) Hecht, D. S.; Thomas, D.; Hu, L.; Ladous, C.; Lam, T.; Park, Y.; Irvin, G.; Drzaic, P. Carbon-Nanotube Film on Plastic as Transparent Electrode for Resistive Touch Screens. *J. Soc. Inf. Disp.* **2009**, *17* (11), 941. https://doi.org/10.1889/JSID17.11.941.

(31) Hu, L.; Hecht, D. S.; Grüner, G. Carbon Nanotube Thin Films: Fabrication, Properties, and Applications. *Chem. Rev.* **2010**, *110* (10), 5790–5844. https://doi.org/10.1021/cr9002962.

(32) Zhou, Y.; Hu, L.; Grüner, G. A Method of Printing Carbon Nanotube Thin Films. *Appl. Phys. Lett.* **2006**, *88* (12), 14–17. https://doi.org/10.1063/1.2187945.

(33) Mustonen, K.; Laiho, P.; Kaskela, A.; Susi, T.; Nasibulin, A. G.; Kauppinen, E. I. Uncovering the Ultimate Performance of Single-Walled Carbon Nanotube Films as Transparent Conductors. *Appl. Phys. Lett.* **2015**, *107* (14), 1–6. https://doi.org/10.1063/1.4932942.

(34) Hussain, A.; Liao, Y.; Zhang, Q.; Ding, E. X.; Laiho, P.; Ahmad, S.; Wei, N.; Tian, Y.; Jiang, H.; Kauppinen, E. I. Floating Catalyst CVD Synthesis of Single Walled Carbon Nanotubes from Ethylene for High Performance Transparent Electrodes. *Nanoscale* **2018**, *10* (20), 9752–9759. https://doi.org/10.1039/c8nr00716k.

(35) Anoshkin, I. V.; Nasibulin, A. G.; Tian, Y.; Liu, B.; Jiang, H.; Kauppinen, E. I. Hybrid Carbon Source for Single-Walled Carbon Nanotube Synthesis by Aerosol CVD Method. *Carbon N. Y.* **2014**, *78*, 130–136. https://doi.org/10.1016/j.carbon.2014.06.057.

(36) Kim, K. K.; Bae, J. J.; Park, H. K.; Kim, S. M.; Geng, H.-Z.; Park, K. A.; Shin, H.-J.; Yoon,

S.-M.; Benayad, A.; Choi, J.-Y.; Lee, Y. H. Fermi Level Engineering of Single-Walled Carbon Nanotubes by AuCl 3 Doping. *J. Am. Chem. Soc.* **2008**, *130* (38), 12757–12761. https://doi.org/10.1021/ja8038689.

(37) Kuang, P.; Park, J.-M.; Leung, W.; Mahadevapuram, R. C.; Nalwa, K. S.; Kim, T.-G.; Chaudhary, S.; Ho, K.-M.; Constant, K. A New Architecture for Transparent Electrodes: Relieving the Trade-Off Between Electrical Conductivity and Optical Transmittance. *Adv. Mater.* **2011**, *23* (21), 2469–2473. https://doi.org/10.1002/adma.201100419.

(38) Saive, R.; Borsuk, A. M.; Emmer, H. S.; Bukowsky, C. R.; Lloyd, J. V.; Yalamanchili, S.; Atwater, H. A. Effectively Transparent Front Contacts for Optoelectronic Devices. *Adv. Opt. Mater.* **2016**, *4* (10), 1470–1474. https://doi.org/10.1002/adom.201600252.

(39) Jiang, S.; Hou, P.-X.; Chen, M.-L.; Wang, B.-W.; Sun, D.-M.; Tang, D.-M.; Jin, Q.; Guo, Q.-X.; Zhang, D.-D.; Du, J.-H.; Tai, K.-P.; Tan, J.; Kauppinen, E. I.; Liu, C.; Cheng, H.-M. Ultrahigh-Performance Transparent Conductive Films of Carbon-Welded Isolated Single-Wall Carbon Nanotubes. *Sci. Adv.* **2018**, *4* (5), eaap9264. https://doi.org/10.1126/sciadv.aap9264.

(40) Khabushev, E. M.; Krasnikov, D. V.; Zaremba, O. T.; Tsapenko, A. P.; Goldt, A. E.; Nasibulin, A. G. Machine Learning for Tailoring Optoelectronic Properties of Single-Walled Carbon Nanotube Films. *J. Phys. Chem. Lett.* **2019**, *10* (21), 6962–6966. https://doi.org/10.1021/acs.jpclett.9b02777.

(41) Rajanna, P. M.; Meddeb, H.; Sergeev, O.; Tsapenko, A. P.; Bereznev, S.; Vehse, M.; Volobujeva, O.; Danilson, M.; Lund, P. D.; Nasibulin, A. G. Rational Design of Highly Efficient Flexible and Transparent P-Type Composite Electrode Based on Single-Walled

Carbon Nanotubes. *Nano Energy* **2020**, *67*, 104183. https://doi.org/10.1016/j.nanoen.2019.104183.

(42) Kim, S. Il; Lee, K. W.; Sahu, B. B.; Han, J. G. Flexible OLED Fabrication with ITO Thin Film on Polymer Substrate. *Jpn. J. Appl. Phys.* **2015**, *54* (9), 090301. https://doi.org/10.7567/JJAP.54.090301.

(43) Fraser, D. B.; Cook, H. D. Highly Conductive, Transparent Films of Sputtered In[Sub 2−x]Sn[Sub x]O[Sub 3−y]. *J. Electrochem. Soc.* **2007**, *119* (10), 1368. https://doi.org/10.1149/1.2403999.

(44) De, S.; King, P. J.; Lyons, P. E.; Khan, U.; Coleman, J. N. Size Effects and the Problem with Percolation in Nanostructured Transparent Conductors. *ACS Nano* **2010**, *4* (12), 7064–7072. https://doi.org/10.1021/nn1025803.

(45) Dresselhaus, M. S.; Jorio, A.; Hofmann, M.; Dresselhaus, G.; Saito, R. Perspectives on Carbon Nanotubes and Graphene Raman Spectroscopy. *Nano Lett.* **2010**, *10* (3), 751–758. https://doi.org/10.1021/nl904286r.

(46) Dresselhaus, M. S.; Dresselhaus, G.; Saito, R.; Jorio, A. Raman Spectroscopy of Carbon Nanotubes. *Phys. Rep.* **2005**, *409* (2), 47–99. https://doi.org/10.1016/j.physrep.2004.10.006.

(47) Behnam, A.; Noriega, L.; Choi, Y.; Wu, Z.; Rinzler, A. G.; Ural, A. Resistivity Scaling in Single-Walled Carbon Nanotube Films Patterned to Submicron Dimensions. *Appl. Phys. Lett.* **2006**, *89* (9), 87–90. https://doi.org/10.1063/1.2339029.

(48) Snow, E. S.; Novak, J. P.; Campbell, P. M.; Park, D. Random Networks of Carbon

Nanotubes as an Electronic Material. *Appl. Phys. Lett.* **2003**, *82* (13), 2145–2147. https://doi.org/10.1063/1.1564291.

(49) Millithaler, J. F.; Reggiani, L.; Pousset, J.; Varani, L.; Palermo, C.; Knap, W.; Mateos, J.; González, T.; Perez, S.; Pardo, D. A Monte Carlo Investigation of Plasmonic Noise in Nanometric N-In 0.53Ga0.47As Channels. *J. Stat. Mech. Theory Exp.* **2009**, *2009* (1). https://doi.org/10.1088/1742-5468/2009/01/P01040.

(50) Kumar, S.; Murthy, J. Y.; Alam, M. A. Percolating Conduction in Finite Nanotube Networks. *Phys. Rev. Lett.* **2005**, *95* (6), 066802. https://doi.org/10.1103/PhysRevLett.95.066802.

(51) Tiedje, T.; Cebulka, J. M.; Morel, D. L.; Abeles, B. Evidence for Exponential Band Tails in Amorphous Silicon Hydride. *Phys. Rev. Lett.* **1981**, *46* (21), 1425–1428. https://doi.org/10.1103/PhysRevLett.46.1425.

(52) Moisala, A.; Nasibulin, A. G.; Brown, D. P.; Jiang, H.; Khriachtchev, L.; Kauppinen, E. I. Single-Walled Carbon Nanotube Synthesis Using Ferrocene and Iron Pentacarbonyl in a Laminar Flow Reactor. *Chem. Eng. Sci.* **2006**, *61* (13), 4393–4402. https://doi.org/10.1016/j.ces.2006.02.020.

(53) Tian, Y.; Timmermans, M. Y.; Kivistö, S.; Nasibulin, A. G.; Zhu, Z.; Jiang, H.; Okhotnikov, O. G.; Kauppinen, E. I. Tailoring the Diameter of Single-Walled Carbon Nanotubes for Optical Applications. *Nano Res.* **2011**, *4* (8), 807–815. https://doi.org/10.1007/s12274-011-0137-6.